

IMECE2009-12643

ON THE FREQUENCY DOMAIN ANALYSIS OF TIRE RELAXATION EFFECTS ON
TRANSIENT ON-CENTER VEHICLE HANDLING PERFORMANCE

Justin Sill

Clemson University- International Center for
Automotive Research
Greenville, SC, US

Beshah Ayalew

Clemson University-International Center for
Automotive Research
Greenville, SC, US

ABSTRACT

This paper presents an elegant frequency domain approach that can be used to analyze lateral vehicle dynamics for transient understeer and oversteer performance. Commonly used steady-state understeer analysis techniques are not able to expose some effects, such as tire relaxation, in on-center transient maneuvers. The approach presented here addresses such transient issues using a simple two degree of freedom handling model coupled to a model for tire lateral dynamics. In addition to the usual yaw rate and lateral acceleration transfer functions, this paper proposes using an understeer angle transfer function as an easy-to-interpret metric to evaluate transient on-center handling. Using the approach, it is shown that at low vehicle velocities, the inclusion of tire relaxation introduces dramatically different system dynamics by introducing highly undamped poles into the coupled system for both an understeering and an oversteering vehicle.

Key Words: transient understeer, tire relaxation, on-center handling, transient handling, vehicle transfer functions, understeer angle

NOMENCLATURE

α_f	Front Tire Slip Angle
α_r	Rear Tire Slip Angle
a	Distance from CG to Front Axle
b	Distance from CG to Rear Axle
A_y	Lateral Acceleration
β	Side Slip
L	Vehicle Wheelbase
λ_f	Front Tire Relaxation Length
λ_r	Rear Tire Relaxation Length
$C_{\alpha f}$	Front Axle Cornering Stiffness
$C_{\alpha r}$	Rear Axle Cornering Stiffness
J_z	Vehicle Yaw Inertia
K_y^f	Front Tire Lateral Stiffness
K_y^r	Rear Tire Lateral Stiffness

m	Vehicle Mass
r	Yaw Rate
V	Vehicle Forward Velocity
δ	Road Wheel Steer Angle Understeer Angle

INTRODUCTION

The lateral stability of vehicles has long been analyzed through simple analytical methods. The dominating approach has been an understeer analysis which can characterize the vehicle's steady-state tendency to understeer or oversteer within the linear handling range [1-6]. The traditional steady-state understeer analysis techniques can aide in the design of the vehicle, the selection of tires, and design of suspension geometry and components. However, these methods exclude transient effects typical of on-center driving, i.e. those characterized by small steering perturbations from straight ahead driving. The realm of on-center handling has become increasingly important because it typifies the most common driving conditions that have low lateral acceleration levels (lower than 0.2 Gs). In such on-center maneuvers, tire relaxation effects play an important role [7], particularly for lower vehicle velocities.

To characterize the on-center transient performance of a vehicle there have been some experimental studies relating the yaw rate and lateral acceleration responses to steering input in order to determine relative understeer/ oversteer changes [8, 9]. Such experimental methods have been successfully used to study the behavior of the entire system, but cannot be used to isolate the effect of tire dynamics on the vehicle performance.

This paper analyzes the transient behavior of on-center handling including tire dynamics. This is done using an elegant frequency domain approach applied to a reduced linear single track model of a two-axle vehicle. In particular, the paper considers the effect of different prevailing lateral tire-relaxation lengths on the front and rear tires of a vehicle on its transient understeer performance.

The rest of the paper is organized as follows. The first section gives a background on the simplified vehicle handling model without tire-relaxation effects. This is then followed by the derivation of the equations for the case with tire-relaxation effects. The models are then simulated mainly in the frequency domain and a discussion is given on two different cases of a nominally understeering and oversteering vehicle. Finally, the observations of the study are summarized in the concluding session of the paper.

BACKGROUND

The Handling Model. The free-body diagram of the widely used handling (bicycle) model is shown in Figure 1 [1, 2, 4-6, 10-13].

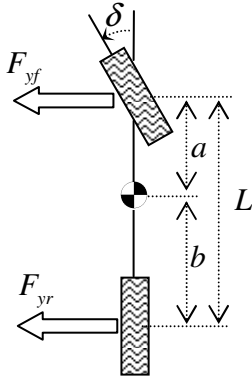


Figure 1. Model Free-Body Diagram

The tire forces are defined by the cornering stiffness and the respective tire slip angles, α_f and α_r , which in turn are functions of vehicle side slip angle, β , yaw rate, r , and road wheel steering angle, δ (see, for example, [4]).

$$F_{yf} = -C_{\alpha_f} \alpha_f \quad (1)$$

$$F_{yr} = -C_{\alpha_r} \alpha_r \quad (2)$$

$$\alpha_f = \beta + \frac{a}{V} r - \delta \quad (3)$$

$$\alpha_r = \beta - \frac{b}{V} r \quad (4)$$

With the side slip angle and the yaw rate as the states of vehicle and with the front road wheel steering angle as input, the equations of motion reduce to:

$$\begin{Bmatrix} \dot{\beta} \\ \dot{r} \end{Bmatrix} = \begin{bmatrix} \frac{-C_{\alpha_f} + C_{\alpha_r}}{mV} & \frac{-aC_{\alpha_f} + bC_{\alpha_r}}{mV^2} - 1 \\ \frac{-aC_{\alpha_f} + bC_{\alpha_r}}{J_z} & \frac{-a^2C_{\alpha_f} + b^2C_{\alpha_r}}{J_z V} \end{bmatrix} \begin{Bmatrix} \beta \\ r \end{Bmatrix} + \begin{bmatrix} \frac{C_{\alpha_f}}{mV} \\ \frac{aC_{\alpha_f}}{J_z} \end{bmatrix} \delta \quad (5)$$

The characteristic equation of this system is given by:

$$\begin{aligned} \Delta_1(s) = & [V^2 m J_z] s^2 \\ & + [mV(C_{\alpha_f} a^2 + C_{\alpha_r} b^2) + V J_z (C_{\alpha_f} + C_{\alpha_r})] s \\ & + [C_{\alpha_f} C_{\alpha_r} L^2 + mV^2 (C_{\alpha_r} b - C_{\alpha_f} a)] \end{aligned} \quad (6)$$

The lateral acceleration and yaw rate transfer functions are determined to be:

$$\frac{A_y}{\delta} = C_{\alpha_f} V \frac{[J_z V] s^2 + [C_{\alpha_r} b L] s + [V C_{\alpha_r} L]}{\Delta_1(s)} \quad (7)$$

$$\frac{r}{\delta}(s) = C_{\alpha_f} V \frac{[amV] s + [C_{\alpha_r} L]}{\Delta_1(s)} \quad (8)$$

These transfer functions can be analyzed to determine a vehicle's handling stability and performance.

Understeer Gradient. In steady-state cornering maneuvers, the above simple model can further be reduced to the determination of the understeer coefficient or gradient, K_{us} . This metric is widely used in determining the oversteering and understeering tendency of vehicles as well as the calculation of critical and characteristic velocities [1, 4-6, 12].

$$K_{us} = \frac{m}{L} \left(\frac{b}{C_{\alpha_f}} - \frac{a}{C_{\alpha_r}} \right) = \frac{\alpha_f - \alpha_r}{A_y} \quad (9)$$

$$V_c = \sqrt{\frac{gL}{|K_{us}|}} \quad (10)$$

The definition of an understeering and oversteering vehicle can be determined from Equation (9). An understeering vehicle has a larger front tire slip angle than that of the rear leading to a positive value for the understeer gradient. Conversely, an oversteering vehicle has a larger rear tire slip angle than that of the front leading to a negative value for understeer gradient.

Experimental Methods. There exist several test methods to quantify transient handling performance of a vehicle. These methods include maneuvers with steer inputs characterized by a step, a sinusoid [14], as well as random or sine sweeps where all frequency ranges are explored [8, 9].

The most used experimental method involves the analysis of a sine sweep maneuver. This maneuver is completed at constant speed and steer amplitude over a range of possible driver input frequencies (approximately 0 to 4 Hz). The time histories of steer angle, yaw rate, and lateral acceleration are processed through FFTs (Fast Fourier Transforms) to yield the vehicle's frequency domain response. This processed data is used to identify four metrics including the vehicle's steady-state yaw rate gain, yaw rate natural frequency, yaw rate damping, and lateral acceleration phase delay at one hertz of steer excitation. These metrics are plotted in a rhombus plot (also known as spider chart) as shown in Figure 2. This is then used to compare relative differences of vehicles or configurations. The tendency of a vehicle, as compared to some baseline (Q), to

be more responsive (P) or more stable (R) can easily be visualized.

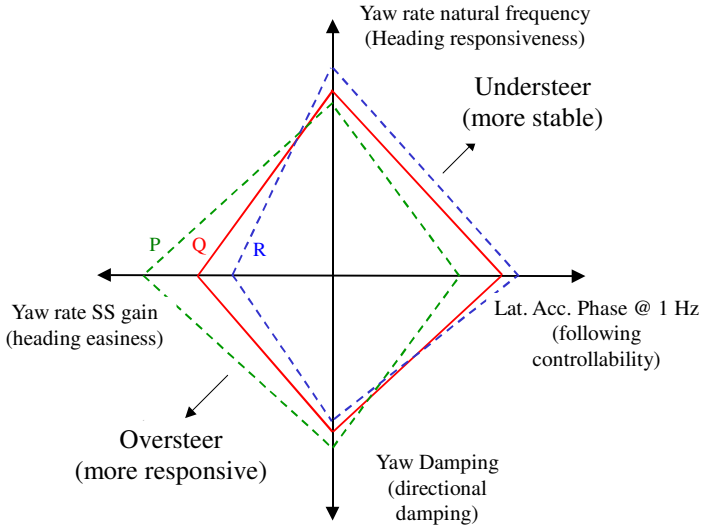


Figure 2. Four Parameter Evaluation Method for Lateral Transient Response [8]

The rhombus plot technique is a powerful tool for analyzing objective test data to determine differences in transient understeer performance for on-center handling and has inspired the frequency domain analysis considered in this paper. The method adopted here enhances the above approach by demonstrating the use of a third transfer function, the understeer angle transfer function. As will be shown below, trends in this transfer function appear easier to interpret.

DERIVATION OF EQUATIONS

The above handling model (lateral & yaw vehicle motions) can be used in conjunction with a first order transient tire model. From Figure 1, the basic equations of motion can be written in the form:

$$mV(\dot{\beta} + r) = F_{yf} + F_{yr} \quad (11)$$

$$J_z \dot{r} = aF_{yf} - bF_{yr} \quad (12)$$

The tire transient behavior is modeled by a first order dynamic system as [15]:

$$\tau_f F_{yf} + F_{yf} = -C_{\alpha f} \alpha_f \quad (13)$$

$$\tau_r F_{yr} + F_{yr} = -C_{\alpha r} \alpha_r \quad (14)$$

Where, the tire time constants τ_f and τ_r are defined by the relaxation length and velocity as [16]:

$$\tau_f = \frac{\lambda_f}{V} \quad (15)$$

$$\tau_r = \frac{\lambda_r}{V} \quad (16)$$

This definition of tire transient behavior was used for simplicity though it should be noted that there are many ways in which to account for tire dynamics including higher order models [4, 7, 17-19]. It should also be noted that when the tire time constants are zero the tires are represented by only cornering stiffnesses and slip angles thus reducing this vehicle model to the traditional steady-state cornering handling model described above.

After substitutions of the time constants and slip angles, the tire force equations can be expressed as shown below:

$$\dot{F}_{yf} = -\frac{C_{\alpha f} V}{\lambda_f} \left(\beta + \frac{a}{V} r - \delta \right) - \frac{F_{yf} V}{\lambda_f} \quad (17)$$

$$\dot{F}_{yr} = -\frac{C_{\alpha r} V}{\lambda_r} \left(\beta - \frac{b}{V} r \right) - \frac{F_{yr} V}{\lambda_r} \quad (18)$$

The complete model can then be represented in state space form with the side slip angle, yaw rate, front axle lateral force, and rear axle lateral force as state variables.

$$\begin{Bmatrix} \dot{\beta} \\ \dot{r} \\ \dot{F}_{yf} \\ \dot{F}_{yr} \end{Bmatrix} = \begin{bmatrix} 0 & -1 & \frac{1}{mV} & \frac{1}{mV} \\ 0 & 0 & \frac{a}{J_z} & -\frac{b}{J_z} \\ -\frac{C_{\alpha f} V}{\lambda_f} & -\frac{C_{\alpha f} Va}{\lambda_f} & -\frac{V}{\lambda_f} & 0 \\ -\frac{C_{\alpha r} V}{\lambda_r} & \frac{C_{\alpha r} Vb}{\lambda_r} & 0 & -\frac{V}{\lambda_r} \end{bmatrix} \begin{Bmatrix} \beta \\ r \\ F_{yf} \\ F_{yr} \end{Bmatrix} + \begin{bmatrix} 0 \\ 0 \\ \frac{C_{\alpha f} V}{\lambda_f} \\ 0 \end{bmatrix} \delta \quad (19)$$

The outputs of interest include the vehicle's side slip, yaw rate, lateral acceleration, and the understeer angle. The lateral acceleration and understeer angle are defined by:

$$A_y = \frac{F_{yf} + F_{yr}}{m} \quad (20)$$

$$UA = \alpha_f - \alpha_r = \left(\beta + \frac{a}{V} r - \delta \right) - \left(\beta - \frac{b}{V} r \right) = \frac{L}{V} r - \delta \quad (21)$$

The understeer angle was derived from the subtraction of the front and rear tire slips angles which in turn are functions of the vehicle side slip angle and location of the vehicle center of gravity as given by Equations (3) and (4). It is interesting to note that the derived understeer angle is related to the yaw rate by the constant ratio of wheelbase to velocity and a shift related to the steer input.

The above output equations as well as the side slip and yaw rate are expressed in terms of state-space output matrices as:

$$\begin{Bmatrix} \beta \\ r \\ A_y \\ UA \end{Bmatrix} = \begin{bmatrix} 1 & 0 & 0 & 0 \\ 0 & 1 & 0 & 0 \\ 0 & 0 & \frac{1}{m} & \frac{1}{m} \\ 0 & \frac{L}{V} & 0 & 0 \end{bmatrix} \begin{Bmatrix} \beta \\ r \\ F_{yf} \\ F_{yr} \end{Bmatrix} + \begin{bmatrix} 0 \\ 0 \\ 0 \\ -1 \end{bmatrix} \delta \quad (22)$$

The transfer functions of the vehicle's lateral acceleration, yaw rate, and understeer angle with respect to steer angle input can be found from this state-space representation of the model.

The characteristic equation of the system in Equation (19) is:

$$\begin{aligned} \Delta_2(s) = & [\lambda_f \lambda_r J_z m] s^4 + [V J_z m (\lambda_f + \lambda_r)] s^3 \\ & + [m(C_{\alpha_f} a^2 \lambda_r + C_{\alpha_r} b^2 \lambda_f) + J_z (C_{\alpha_f} \lambda_r + C_{\alpha_r} \lambda_f) + V^2 m J_z] s^2 \quad (23) \\ & + [mV(C_{\alpha_f} a(a - \lambda_r) + C_{\alpha_r} b(b + \lambda_f)) + V J_z (C_{\alpha_f} + C_{\alpha_r})] s \\ & + [C_{\alpha_f} C_{\alpha_r} L^2 + mV^2 (C_{\alpha_r} b - C_{\alpha_f} a)] \end{aligned}$$

The yaw rate, lateral acceleration, and understeer angle transfer functions are given, respectively, by:

$$\frac{r}{\delta}(s) = C_{\alpha_f} V \frac{[am\lambda_r]s^2 + [amV]s + [C_{\alpha_r}L]}{\Delta_2(s)} \quad (24)$$

$$\frac{A_y}{\delta}(s) = C_{\alpha_f} V \frac{[J_z \lambda_r]s^3 + [J_z V]s^2 + [C_{\alpha_r} b L]s + [V C_{\alpha_r} L]}{\Delta_2(s)} \quad (25)$$

$$\begin{aligned} \frac{UA}{\delta}(s) = & \frac{[-mJ_z \lambda_f \lambda_r]s^4 + [-mJ_z V (\lambda_f + \lambda_r)]s^3 \\ & + [mb(C_{\alpha_f} a \lambda_r - C_{\alpha_r} b \lambda_f) - J_z (C_{\alpha_f} \lambda_r + C_{\alpha_r} \lambda_f + mV^2)]s^2 \\ & + [mV(C_{\alpha_f} a(\lambda_r + b) - C_{\alpha_r} b(\lambda_f + b)) - J_z V (C_{\alpha_f} + C_{\alpha_r})]s \\ & + [C_{\alpha_f} mV^2 (a - b)]}{\Delta_2(s)} \quad (26) \end{aligned}$$

For comparison, the understeer angle with respect to steer angle transfer function for the model without relaxation (without tire dynamics) is defined here by:

$$\begin{aligned} \frac{UA}{\delta}(s) = & \frac{[-mJ_z V^2]s^2 \\ & + [mVb(C_{\alpha_f} a - C_{\alpha_r} b) - J_z V (C_{\alpha_f} + C_{\alpha_r})]s \\ & + [C_{\alpha_f} mV^2 (a - b)]}{\Delta_1(s)} \quad (27) \end{aligned}$$

It should be noted that when the relaxation length of the front and rear tires are set to zero the model with relaxation lengths will reduce to the vehicle model without relaxation.

RESULTS & DISCUSSION

In this section, the transfer functions derived above are used to study the transient response of the vehicle. An understeering as well as an oversteering vehicle with different rear tire cornering stiffnesses are analyzed. The relevant values are given in Table 1.

Table 1. Vehicle Parameters

Parameter	Value		Units
	Understeer	Oversteer	
Vehicle Mass	1581		kg
Yaw Inertia	2686		kg-m ²
Wheelbase	2.7		m
Weight Distribution	63/37		%
Tire Lateral Stiffness	150		N/mm
Front Tire Cornering Stiffness	1504		N/deg
Front Relaxation Length	0.575		m
Rear Tire Cornering Stiffness	1043	687	N/deg
Rear Relaxation Length	0.398	0.262	m
Understeer Gradient	4.83	-9.17	deg/G
Characteristic/Critical Velocity	200	145	kph

The relaxation lengths for the front and rear tires were calculated based on a tire lateral stiffness for the front and rear tires as well as the respective cornering stiffnesses.

$$\lambda_f = \frac{C_{\alpha_f}}{K_{yf}} \quad (28)$$

$$\lambda_r = \frac{C_{\alpha_r}}{K_{yr}} \quad (29)$$

Note that the tire stiffnesses, K_{yf} & K_{yr} , are the same values for both front and rear axles. This assumption of the insensitivity of lateral stiffness to load as compared to cornering stiffness (due to the dominant effect of structural tire components [16]), yields different relaxation lengths for the front and rear axles for both vehicles, because of its dependency on cornering stiffness in Equations 28 & 29.

Understeering Vehicle. The understeer vehicle, as defined in Table 1, was analyzed using the models developed above with and without tire relaxation. The yaw rate and lateral acceleration transfer functions, defined in Equations (7, 8, 24, & 25), for various vehicle speeds, including 30, 60, 90, 120, & 150 kph, are shown in Figures 3&4.

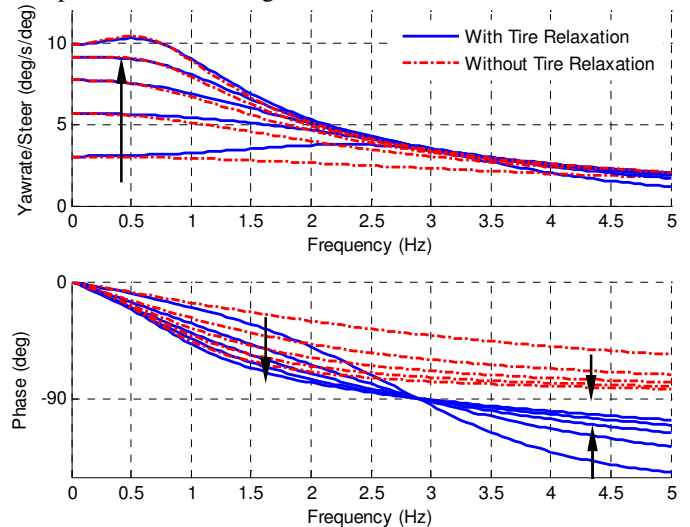


Figure 3. Yaw Rate Transfer Function of Understeering Vehicle with and without Tire Relaxation for Increasing Velocity (Arrows)

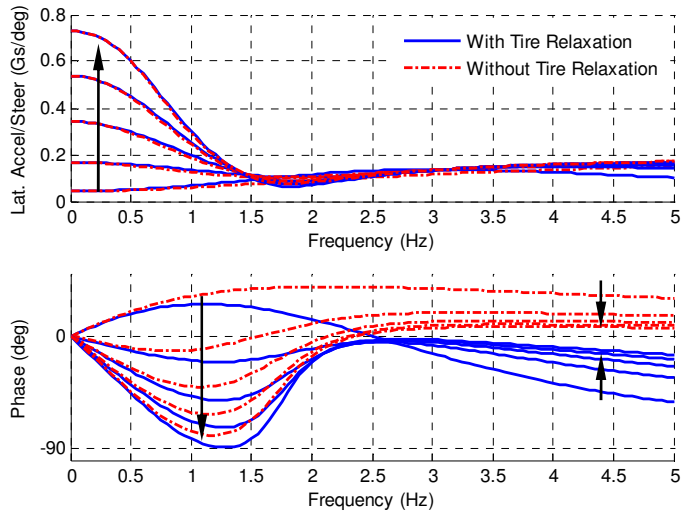


Figure 4. Lateral Acceleration Transfer Function of Understeering Vehicle with and without Tire Relaxation for Increasing Velocity (Arrows)

As can be seen from the figures, the magnitude and phase delay for the model with and without tire relaxation does show some differences. For low frequencies, below 0.5 Hz, the models show similar response, however for higher frequencies the phasing is dramatically different. It is difficult to interpret these differences and their significance from the perspective of a driver. So it is proposed to use the unconventional understeer angle transfer function, defined in Equations (26 & 27), to investigate the model performance (See Figure 5).

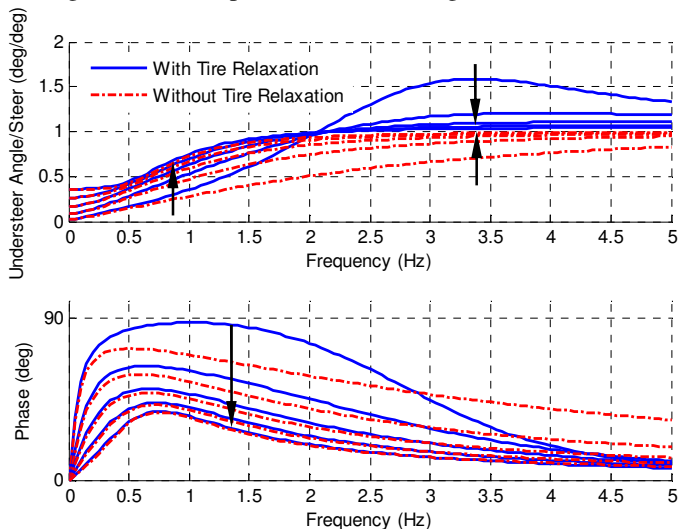


Figure 5. Understeer Angle Transfer Function of Understeering Vehicle with and without Tire Relaxation for Increasing Velocity (Arrows)

It can be observed that the understeer angle approaches a magnitude of one degree per degree of steering for high frequencies. The low or near zero values of yaw rate at such frequencies causes the understeer angle to approach the steering input. This is because, at high frequencies, the understeer angle becomes a function of primarily the front tire slip angle which in turn approaches the steer angle as both the yaw rate and the

vehicle side slip angle vanishes. The rear tire slip angle also approaches zero. This is evident from Equations (3) and (4).

The effect of tire relaxation on the understeer angle of the vehicle is more evident at low vehicle speeds, as can be seen by the difference in the models at the lowest speed of 30 kph. As the velocity is increased, the understeer response of the model including tire relaxation approaches that of the model excluding tire relaxation.

It can also be observed that the understeer transfer function shows a peak frequency at low velocities that could be significant. This peak is located at 3-3.5 Hz at 30 kph, which lies in a frequency range in which a driver maybe sensitive. It can also be observed that the model with relaxation length has values of understeer angle greater than one for frequencies above 2 Hz. This indicates an increased measure of understeer when tire relaxation is included.

The effect of velocity on tire relaxation can be further analyzed by computing the poles of the characteristic equations (6) and (23) for increasing velocity. The loci of the poles of the model with and without tire relaxation are shown in Figure 6. As expected for an understeering vehicle, the model without tire relaxation includes only two imaginary poles [4]. However, the model with relaxation transitions from four imaginary poles to two imaginary and two real ones as the vehicle velocity is increased.

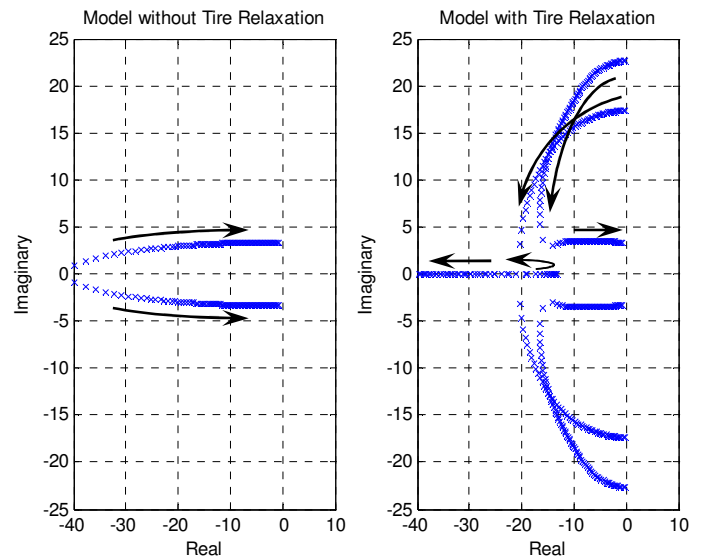


Figure 6. Loci of the Poles for Understeering Vehicle with and without Tire Relaxation for Increasing Velocity (Arrows)

The effect of relaxation length is reduced as velocity increases as shown by the convergence of the left and right plots to similar imaginary poles. This is consistent with previous studies showing that the effect of tire relaxation on vehicle handling is most important at low velocities [7].

The initial imaginary poles (near zero velocity) that are on the imaginary axis for low speeds are quite different from the poles of the model without tire relaxation. The characteristic

equation (23) with tire relaxation as the velocity approaches zero reduces to:

$$\Delta_2(V \rightarrow 0) = [\lambda_f \lambda_r J_z m] s^4 + [m(C_{\alpha_f} a^2 \lambda_r + C_{\alpha_r} b^2 \lambda_f) + J_z(C_{\alpha_f} \lambda_r + C_{\alpha_r} \lambda_f)] s^2 + [C_{\alpha_f} C_{\alpha_r} L^2] \quad (30)$$

It can be shown that the roots of this equation are pure imaginary for the data in Table 1 verifying the above observation that at low speeds, tire-relaxation introduces dominant oscillations. The impact of the system poles can further be seen in the vehicle's response to a step steer maneuver of one degree road wheel angle at increasing velocities of 30, 60, 90, & 120 kph (Figure 7).

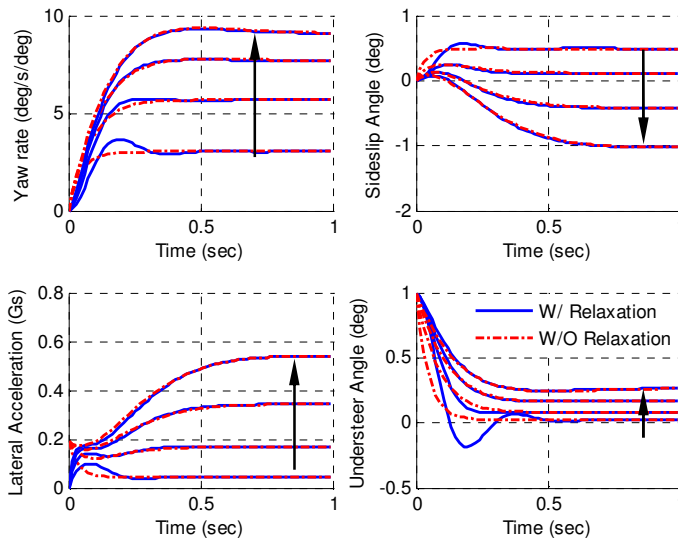


Figure 7. Understeering Vehicle Response to Step Steer Input for Increasing Velocities (Arrows)

As can be seen from the response, the model with relaxation exhibits more oscillation at low speeds compared to the model without relaxation. Interestingly, this oscillation causes the understeer angle to become negative for the speed of 30 kph, as the yaw rate overshoots its steady-state value.

Oversteering Vehicle. The oversteering vehicle, as defined by the parameters in Table 1, was analyzed similarly. The yaw rate and lateral acceleration transfer functions for a few selected velocities (30, 60, 90, & 120 kph) are shown in Figures 8 & 9, respectively.

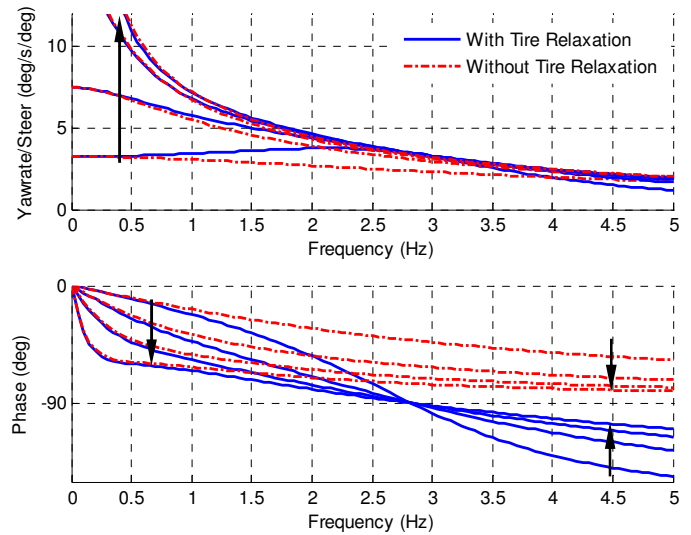


Figure 8. Yaw rate Transfer Function of Oversteering Vehicle with and without Tire Relaxation for Increasing Velocity (Arrows)

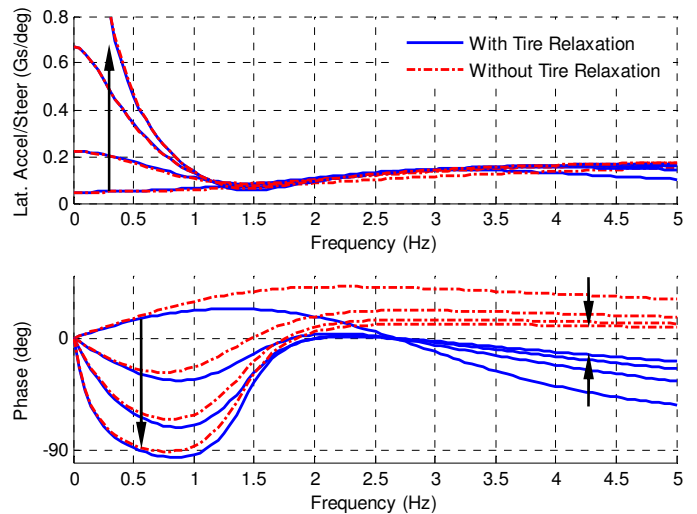


Figure 9. Lateral Acceleration Transfer Function of Oversteering Vehicle with and without Tire Relaxation for Increasing Velocity (Arrows)

The yaw rate and lateral acceleration response looks similar to the previous case with the exception of steady-state performance. The yaw rate and lateral acceleration gain increase greatly as the velocity is increased as expected for an oversteering vehicle [1, 4, 5].

The understeer angle transfer function for the oversteering vehicle is shown in Figure 10. The steady-state understeer angle is 180 degrees out-of-phase with respect to the steering input. This is consistent with the expected negative value of understeer angle for an oversteering vehicle.

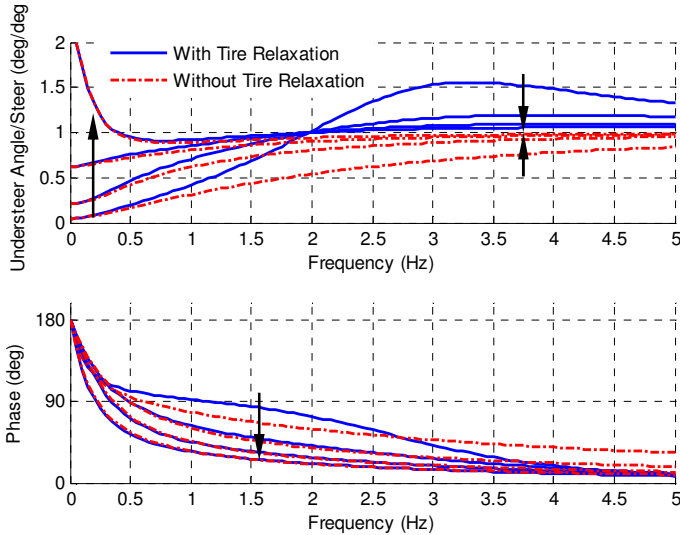


Figure 10. Understeer Angle Transfer Function of Oversteering Vehicle with and without Tire Relaxation for Increasing Velocity (Arrows)

It is also noteworthy that the asymptotes of magnitude and phase of the oversteering vehicle are identical to that of the understeering vehicle in Figure 5. Therefore, for the oversteering and understeering vehicles the understeer performance for increasing frequencies of excitation converge to pure understeer as seen by an understeer angle of one degree per degree of steering.

The loci of the poles for the oversteering vehicle over a range of increasing velocities are shown in Figure 11.

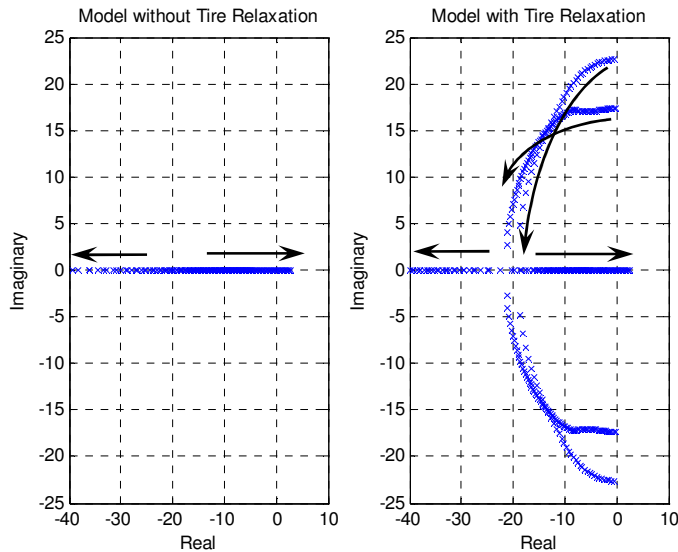


Figure 11. Loci of Poles for Oversteering Vehicle with and without Tire Relaxation for Increasing Velocity (Arrows)

The model without relaxation, including two negative real poles, reaches instability when one of the poles crosses the imaginary axis. The loci of the poles for the model with relaxation progressively move from four imaginary poles to four real poles for increasing velocity as shown by the arrows in

Figure 11. Accordingly, at low vehicle velocities there exist two distinct frequencies of oscillation. Similarly to the model without relaxation, one of these poles crosses the imaginary axis at a critical velocity inducing instability. Note that at high velocities, the two models converge to each other meaning that tire relaxation does not dramatically reduce the critical velocity.

The step steer response for the oversteering vehicle, showing the yaw rate, side slip angle, lateral acceleration, and understeer angle is shown in Figure 12.

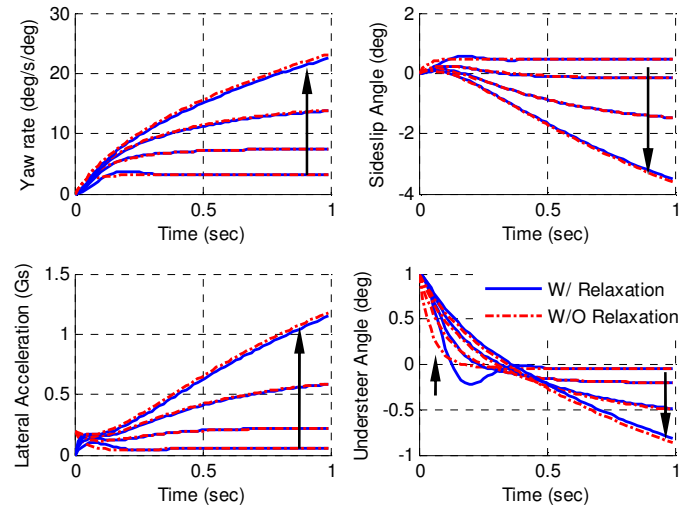


Figure 12. Oversteering Vehicle Response to Step Steer Input for Increasing Velocities (Arrows)

The model with relaxation length again shows oscillation at lower vehicle speeds, particularly on the understeer angle. The usefulness of the understeer angle as a response is shown by how it reveals the most dramatic differences in performance, especially at lower vehicle speeds.

CONCLUSIONS

In this work, transient understeer performance of a vehicle was analyzed using a frequency domain approach. The effects of tire relaxation on transient handling performance is shown through an analysis of an understeering and oversteering vehicle using transfer functions and complex plane locus of the system poles for the models. The following observations were made from the analysis:

- Relaxation length produces larger magnitude ratios for the understeer angle transfer function for both vehicles.
- For increasing velocity, a locus of the poles analysis shows that the poles of the model with tire relaxation converge to poles of the model without relaxation. In other words, the most dramatic effects of tire relaxation are apparent at low velocities, where highly oscillatory poles are introduced by tire relaxation for both oversteering and understeering vehicles.
- Relaxation length does not significantly affect the stability or critical velocity magnitude of the studied

oversteering vehicle, due to the reduced effect of relaxation at such a velocity (145 kph).

- For increasing excitation frequencies, an understeering and oversteering vehicle converge to pure understeer as measured by a one degree understeer angle per degree of steering.
- As expected, the steady-state performance of a model with and without tire relaxation are identical, i.e, in steady-state tire relaxation has no effect on the response of the vehicle.

It is also proposed in this paper that the understeer angle transfer function makes for an easy to interpret parameter for such on-center analyses.

REFERENCES

1. Gillespie, T., *Fundamentals of Vehicle Dynamics*. 1992: Society of Automotive Engineers.
2. Karogal, I. and B. Ayalew. *Independent Torque Distribution Strategies for Vehicle Stability Control*. in *World Congress of the Society of Automotive Engineers*. 2009. SAE Paper No. 09AC-0075. Detroit, MI: SAE, Inc.
3. Karogal, I., B. Ayalew, and H. Law. *An Iterative Approach for Steady State Handling Analysis of Vehicles*. in *Proceedings of the ASME 2008 International Design Engineering Technical Conferences & Computers and Information in Engineering Conference*. 2008. ASME Paper No. DETC2008-50033. New York, NY: ASME.
4. Genta, G., *Motor Vehicle Dynamics: Modeling and Simulation*. Series on Advances in Mathematics for Applied Sciences. Vol. 43. 1997, Singapore: World Scientific Publishing.
5. Milliken, W.M.a.D., *Race Car Vehicle Dynamics*. 1995, Warrendale, PA: Society of Automotive Engineers, Inc.
6. Wong, J.Y., *Theory of Ground Vehicles*. 1993, New York, NY: John Wiley & Sons.
7. Heydinger, G., W.R. Garrott, and J.P. Chrstos. *The Importance of Tire Lag on Simulated Transient Vehicle Response*. in *World Congress of the Society of Automotive Engineers*. 1991. SAE Paper No. 910235. Detroit, MI: SAE, Inc.
8. Mimuro, T., et al. *Four Parameter Evaluation Method of Lateral Transient Response*. in *World Congress of the Society of Automotive Engineers*. 1990. SAE Paper No. 901734: SAE, Inc.
9. Huang, F., J.R. Chen, and L.-W. Tsai. *The Use of Random Steer Test Data for Vehicle Parameter Estimation*. in *World Congress of the Society of Automotive Engineers*. 1993. SAE Paper No. 930930. Detroit, MI: SAE, Inc.
10. Sill, J., *Modeling, Testing, and Analysis of On-center Handling for Mid-Size Sport Utility Vehicles*, Master Thesis in *Mechanical Engineering*. 2006, Clemson University: Clemson, SC.
11. Ghoneim, Y., et al., *Integrated Chassis Control System to Enhance Vehicle Stability*. *International Journal of Vehicle Design*, 2000. **Vol. 23**: p. 124-144.
12. Karnopp, D., *Vehicle Stability*. 2004: CRC Press.
13. Mouri, H., M. Kubota, and N. Horiguchi. *Study on Effects of Transient Steering Efforts Characteristics on Driver's Steering Behavior*. in *World Congress of the Society of Automotive Engineers*. 2007. SAE Paper No. 2007-01-0823. Detroit, MI: SAE, Inc.
14. Norman, K. *Objective Evaluation of On-center Handling Performance*. in *World Congress of the Society of Automotive Engineers*. 1984. SAE Paper No. 840069. Detroit, MI: SAE, Inc.
15. Rill, G. *First Order Tire Dynamics*. in *European Conference on Computational Mechanics*. 2006. Lisbon, Portugal.
16. Rhyne, T., *Class Notes on Tire Behavior*. 2009, Clemson University - International Center for Automotive Research.
17. Pacejka, H., *Tyre and Vehicle Dynamics*. 2002: Oxford: Butterworth-Heinemann.
18. Hou, Y., et al. *A Study of Tire Lag Property*. in *World Congress of the Society of Automotive Engineers*. 2001. SAE Paper No. 2001-01-0751. Detroit, MI: SAE, Inc.
19. Bergman, W. and C. Beauregard. *Transient Tire Properties*. in *Automotive Engineering Congress and Exposition*. 1974. SAE Paper No. 740068. Detroit, MI: SAE, International.